



TITLE:

# The Effects of Foreign Metallic Ions in the Electrolyte upon the Inner Structure of Electrolytic White Tin

AUTHOR(S):

Hirata, Hideki; Koto, Hajime; Shimizu, Etsu

---

CITATION:

Hirata, Hideki ...[et al]. The Effects of Foreign Metallic Ions in the Electrolyte upon the Inner Structure of Electrolytic White Tin. *Memoirs of the College of Science, Kyoto Imperial University. Series A* 1939, 22(3): 209-223

ISSUE DATE:

1939-05-31

URL:

<http://hdl.handle.net/2433/257220>

RIGHT:

# The Effects of Foreign Metallic Ions in the Electrolyte upon the Inner Structure of Electrolytic White Tin<sup>1</sup>

By Hideki Hirata, Hajime Kotô and Etsu Shimizu

(Received April 20, 1939)

## Abstract

The crystalline configurations of a few electrolytic specimens of white tin, deposited from solutions containing a small quantity of  $\text{Fe}^{++}$  and  $\text{Mn}^{++}$  ions respectively in addition to  $\text{Sn}^{++}$  ions, were examined with X-rays. Supplementary to these specimens, the inner structure of an electrolytic deposition obtained with a solution containing a small quantity of  $\text{Cu}^{++}$  ions beside  $\text{Sn}^{++++}$  ions, was also examined. To make clear the effects of the aforesaid foreign metallic ions upon the crystalline configuration of electrolytic white tin, the experimental results thus obtained were compared with those of the previous researches,<sup>2</sup> carried out utilizing as the electrolytes some stannous or stannic solutions free from any metallic impurity. The considerations consequent upon this comparison, led us to conclude on the one hand, that the presence of  $\text{Fe}^{++}$  and  $\text{Mn}^{++}$  ions in the electrolytes converts the direction of the maximum growth of the deposited tin, in a way similar to the case of the alternation of the ionic valency of Sn observed in the previous researches; while, on the other hand, the direction of the common axis of micro-crystals in electrolytic specimens of white tin having a fibrous nature, was found usually to vary according to the presence of  $\text{Fe}^{++}$  ions in the electrolytes, though the direction of the fibre remains unaffected by the presence of  $\text{Mn}^{++}$  or  $\text{Cu}^{++}$  ions. Moreover, it was thought quite possible that the electrolytic deposition containing 96.8% of Sn and 3.2% of Cu examined in the present experiment, is only an aggregation of crystals of white tin interspersed with colloidal particles containing Cu atoms.

## Introduction

A number of X-ray examinations of the inner structure of electrolytic metals, have already been carried out by Glocker, Kaupp<sup>3</sup> and many others.<sup>4</sup> As a consequence of these examinations, not only the crystalline configurations of various electrolytic metals, but their varia-

1. This was read at the meeting of the Institute for Metals of Japan, April, 1938.
2. H. Hirata, H. Komatsubara and Y. Tanaka; The Anniversary Volume dedicated to Prof. Masumi Chikashige, 261 (1930).  
H. Hirata and Y. Tanaka; These Memoirs, A, 17, 143 (1934).
3. R. Glocker & E. Kaupp; Zeits. f. Phys., 24, 21 (1924).
4. e. g., R. M. Bozorth; Phys. Rev., 26, 390 (1925).  
P. K. Frohlich, G. L. Clark & R. A. Aborn; Zeits. f. Elek. Chem., 32, 295 (1926).

tions owing to the difference in the current density between two electrodes, the chemical valency of the metallic ions, etc., given rise to by the condition of the electrolysis, have also become clear to a certain extent. But it was found by T. Nomitsu<sup>1</sup> a few years ago, that the macro-structure of electrolytic metals is greatly affected by the presence of some foreign metallic ions in the electrolyte. Thus the conclusions drawn from the results of the aforesaid X-ray examinations, which dealt mainly with specimens obtained by utilizing as the electrolytes metallic solutions free from any foreign metallic ion, can hardly be thought to give satisfactory information in connection with the inner structure of the electrolytic specimens of metals, deposited by the presence of foreign metallic ions in the electrolyte. So the writers were led to perform the present experiment, not only by way of continuing the foregoing researches on the crystalline configuration of several electrolytic metals carried out in our laboratory,<sup>2</sup> but as a preliminary examination on the idiosyncrasies of the growth of the electrolytic alloys; the study was made on two kinds of specimens of electrolytic white tin (called for convenience Specimen A and Specimen B) deposited from stannous solutions containing a small quantity of ferrous and of manganous ions respectively. Supplementary to these specimens, the inner structure of an electrolytic deposition (called Specimen C) obtained with a solution containing a small quantity of cupric ions beside stannic ions was also investigated.

In the present experiment, the crystalline configurations of the specimens were examined by the Laue method similarly as in the former ones, utilizing mainly the heterogeneous X-ray emitted from the molybdenum anticathode. Furthermore, examination of the crystal structure of some of the specimens, was also carried out with the monochromatic X-ray (Mo  $K\alpha$  radiation) by the powder method. To obtain the Laue photographs, the photographic films were always placed perpendicular to the incident X-ray beam, 3 cms. behind the specimen: While the powder photographs of the specimens were taken with a cylindrical camera 16 cms. in diameter. The experimental results thus obtained will be described below.

---

1. unpublished.

2. e. g., H. Hirata and H. Komatsubara; *Zeits. f. Anorg. u. Allgem. Chem.*, **158**, 137 (1926).

H. Hirata and Y. Tanaka: *These Memoirs*, **11**, 429 (1928), **15**, 9 (1932).

S. Yamamori and S. Yoshimoto; *These Memoirs*, **21**, 75 (1938).

### Specimens

Among the specimens used in the present experiment, Specimens A and B were prepared by T. Nomitsu at the Watanabe Laboratory of the Institute for Chemical Research of Kyoto Imperial University, employing essentially the same procedure that has already been described in these memoirs.<sup>1</sup> Consequently a brief summary confined to the points that were altered in the present case, will suffice here.

To prepare the electrolyte for these specimens, a small quantity of ferrous sulphate ( $\text{FeSO}_4 \cdot 7\text{H}_2\text{O}$ ) or manganous sulphate ( $\text{MnSO}_4 \cdot 5\text{H}_2\text{O}$ ) was respectively added to a sulphuric acid solution of stannous sulphate (a solution obtained by dissolving  $\text{SnSO}_4$  in a mixture of 1 litre of  $\text{H}_2\text{O}$  and 20 c.c. of conc.  $\text{H}_2\text{SO}_4$ ). It was noticed that in the electrolyte, the ions of Sn were reported to exist mostly (over 90%) in the stannous form. The conditions under which the specimens were deposited from these electrolytes, are given below:—

Composition of metallic ions in the electrolyte: Sn about 5 gm./100 c.c., Fe about 3~5 gm./100 c.c.

Cathode: lead plate 2.5 cm.  $\times$  6 cm. in area.

Anode: tin plate 5 cm.  $\times$  6 cm. in area.

Current density: 0.008 amp./ $\text{cm}^2$ . (in front of the cathode).

Terminal voltage: 2.35~2.65 volts.

Temperature: 22°~25°C.

As the result of the electrolysis above mentioned, the specimens of white tin came to appear in an acicular form (0.8~1.2 mm. in diameter), usually having the largest surface parallel to the stem of the acicula. The micro-structure of some of these specimens is reproduced in Figs. 1~4, Plate I.

Specimen C used in the present experiment together with these two kinds of specimens, A and B, was prepared at the laboratory of the Imperial Mint, Osaka, by one of the writers. To obtain this specimen, the deep blue solution containing  $\text{Cu}(\text{HN}_3)_4^{++}$  ions<sup>2</sup> was decolorized by adding potassium cyanide (KCN) and then mixed with the solution of sodium stannate ( $\text{Na}_2\text{SnO}_3 \cdot 3\text{H}_2\text{O}$ )<sup>3</sup>, before it was utilized

---

1. Loc. cit.

2. To prepare this solution,  $\text{CuCO}_3$  was first precipitated from the water solutions of  $\text{CuCl}_2$  by adding  $\text{K}_2\text{CO}_3$ . Then, the precipitation of the carbonate thus deposited, was resolved with  $\text{NH}_4\text{OH}$ .

3. To prepare this solution,  $\text{SnCO}_3$  was first precipitated from the water solution of  $\text{SnCl}_2 \cdot 2\text{H}_2\text{O}$  by adding  $\text{K}_2\text{CO}_3$ . Then the precipitation of the carbonate thus deposited, was resolved with  $\text{NaOH}$ .

as the electrolyte. From the electrolyte above mentioned, Specimen C was deposited under the following conditions.

Composition of metallic ions in the electrolyte : Sn 2.40 gm./100 c.c.

Cu 0.80 gm./100 c.c.

Cathode : platinum plate 1 cm.  $\times$  1.5 cm. in area.

Anode : bronze plate (containing 60% of Sn and 40% of Cu)  
5 cm.  $\times$  10 cm. in area.

Current density : 0.005~0.008 amp./cm.<sup>2</sup>

Terminal voltage : 0.3~0.5 volts.

Temperature : room temperature.

The micro-structure of Specimen C deposited by the aforesaid procedure was found, as can be seen in Fig. 5, Plate I, to be entirely different from those of Specimens A and B. This specimen took the form of a dendrite instead of an acicula. Furthermore, it was noticed that Specimen C is not completely made up of pure Sn as are Specimens A and B, but is composed of 96.8% of Sn and 3.2% of Cu. Thus, Specimen C may be looked upon as a sort of alloy.

### Experimental Results

(i) Specimen A. From a fragment of Specimen A defined above, the diffraction pattern was taken, by setting the largest surface perpendicular to the incident X-ray beam. The diffraction patterns thus obtained, are usually seen to be essentially the same, as reproduced in Fig. 6, Plate I. But here and there, occasionally some exceptions were detected. Besides the patterns consisting of a few Laue's spots (see Fig. 6), figures made up of a set of more Laue's spots or a number of short radiating bands, as shown in Figs. 7 and 8, Plate I, were also found to be given rise to by some specimens. Furthermore, with a few specimens, we obtained diffraction figures consisting of an assemblage of numerous elongated Laue's spots, as reproduced in Fig. 9, Plate I. Here it must be remarked that the direction of the maximum growth of the deposited tin, was always taken vertically.

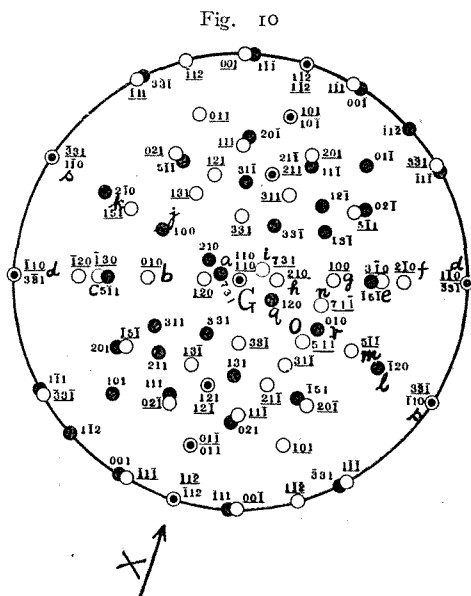
Having thus confirmed these facts, the writers tried by the aid of an improved Yoshida's crystallographic scale<sup>1</sup>, to determine the crystalline configurations corresponding to the various figures. From the results thus determined, the pattern in Fig. 6, Plate I was found to

---

1. U. Yoshida; Japanese J. Phys., 4, 133 (1927) and S. Takeyama; These Memoirs, A, 11, 467 (1928).

be caused by two crystals of white tin, situated with reference to each other, in the way represented in the annexed figure, Fig. 10.

In Fig. 10, various atomic planes belonging to these two crystals are projected by the stereographic method.<sup>1</sup> To distinguish the atomic planes of one of these crystals from those of the other, their points of projection are indicated in Fig. 10 by white circles, and those corresponding to the other by black ones. The point G in this figure is the projection of the vertical direction in Fig. 6, Plate I, which coincides with the longitudinal axis of the specimen. Furthermore, the small letters *a*, *b*, *c*, ..., *q*, *r*, *s* in Fig. 10 mark respectively the atomic planes, which were found to give rise to the Laue spots represented by the same letters in Fig. 6, Plate I, when the incident X-ray beam was made to strike the specimen perpendicularly to its longitudinal axis, taking the direction parallel to the arrow X.<sup>2</sup> As



may be seen from Fig. 10, the two crystals of white tin in Specimen

1. It is generally accepted that the crystal of white tin belongs to the tetragonal system of a proper structure (white tin type structure), having 4 atoms in its unit cell, the length of the lateral and vertical axes of this cell being  $a_0 = 5.819 \text{ \AA}$ . and  $c_0 = 3.175 \text{ \AA}$ . respectively. But in this paper, following A. E. van Arkel [Proc. Roy. Acad. (Amsterdam), 27, 97 (1924)] crystallographic indices are designated with a different co-ordinate system, as it seems to be convenient in comparing the results of the present experiment with these obtained in the previous ones, as well as with various mineralogical arguments. According to the above designation, the crystal of white tin is described as belonging to the tetragonal system of a diamond-type structure, having 8 atoms in its unit cell: The length of the lateral axis of such a cell amounts to  $a_0 = 8.228 (\div 5.819 \times \sqrt{2}) \text{ \AA}$  instead of  $a_0 = 5.819 \text{ \AA}$ ., while that of the vertical axis remains  $c_0 = 3.175 \text{ \AA}$ . the same as is generally accepted.

2. The following correspondence was found to exist between the Laue spots in Fig. 6, Plate I and the indices of the atomic planes of these two crystals:—

*a*,  $73\bar{1}$ ; *b*,  $0\bar{1}0$ ; *c*,  $1\bar{3}0$ ; *d*,  $1\bar{1}0$ ; *e*,  $3\bar{1}0$ ; *f*,  $1\bar{7}1$ ; *g*,  $100$ ; *h*,  $210$ ; *i*,  $731$ ; *j*,  $100$ ; *k*,  $2\bar{1}0$  &  $151$ ; *l*,  $1\bar{2}0$ ; *m*,  $5\bar{1}1$ ; *n*,  $7\bar{1}1$ ; *o*,  $5\bar{1}\bar{1}$ ; *p*,  $75\bar{1}$ ; *q*,  $120$ ; *r*,  $010$ ; *s*,  $1\bar{1}0$ .

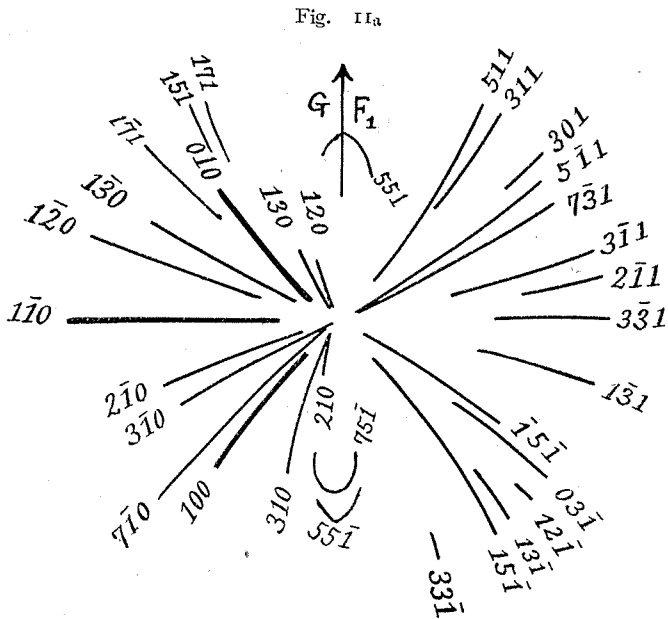
$A_1$ , with which Fig. 6, Plate I was obtained, can be considered to be so situated that each of them has one of its (110) planes in the direction perpendicular to the axis of the acicula, and one of its (211) planes in the direction parallel to the largest face of the specimen.

Having ascertained these facts with regard to Specimen  $A_1$ , the writers tried to determine the crystalline configuration of Specimen  $A_2$ , which gave rise to Fig. 7, Plate I. This determination was made at the outset, by comparing Fig. 6, Plate I with Fig. 7, Plate I. By this comparison, it was easily seen that the diffraction pattern in the former figure, Fig. 6, was not essentially the same with, but a part of the pattern in the latter one, Fig. 7: i. e., although all the Laue spots in Fig. 6 can also be detected in Fig. 7, yet they do not always appear in the former figure according to their intensity in the latter one, some very intense spots in the latter being absent in the former. Thus, we may presume that a considerable part of Specimen  $A_2$ , which gave rise to the latter figure, Fig. 7, Plate I, partakes of the same crystalline configuration as Specimen  $A_1$  corresponding to the former one, Fig. 6, Plate I.

By calculation it was confirmed that Specimen  $A_2$  is made up of the aggregation of three similar crystalline configurations, each one of them being the same as that in Specimen  $A_1$ . To state it more precisely, one of these configurations was seen to have the orientation to the incident X-ray beam suggested by Fig. 10, while two others were found to rotate around the axis of the acicula [one of the normals to the atomic planes (110) marked G in Fig. 10] from the original orientation above mentioned, by the angles  $3^\circ$  and  $2^\circ$  in the counter-clockwise and the clockwise senses respectively.

Furthermore, diffraction patterns explainable by considerations nearly the same as before, can also be observed in Fig. 8, Plate I, which was given rise to by Specimen  $A_3$ . It goes without saying that a diffraction pattern consisting of a set of short radiating bands as seen in Fig. 8, can only appear from a specimen of a fibrous structure, in which the micro-crystals are rotated within a certain angle around their common axis. By making use of the crystallographic scale again, the diffraction pattern reproduced in Fig. 8, Plate I was ascertained to be given rise to by the incomplete rotation of two sets of the micro-crystals of white tin around the longitudinal axis of Specimen  $A_3$ , the micro-crystals in each set being situated in relation to each other as is indicated by Fig. 10. The reasoning which leads to this conclusion is briefly given below.

Let us suppose that the micro-crystals in Specimen  $A_3$  have two original orientations to the incident X-ray beam, as is expressed by two sets of small circles in Fig. 10; then the theoretical distribution of the radiating bands given rise to by the incomplete rotations of the micro-crystals around a definite common axis, would be represented by a superposition of two figures, the one shown in Fig. 11<sub>a</sub> being produced by a set of atomic planes corresponding to the black circles



in Fig. 10, and the other shown in Fig. 11<sub>b</sub>, by those corresponding to the white ones. To draw Fig. 11<sub>a</sub>, the micro-crystals were assumed to rotate to the angles of  $20^\circ$  and  $15^\circ$  in the counter-clockwise and the clockwise sense respectively from the original orientation above stated, around one of the normals of (110) planes, represented by G in Fig. 10: While Fig. 11<sub>b</sub> was drawn by taking the angle of the rotation as  $55^\circ$  in the clockwise sense around the same axis. In Fig. 12, the theoretical positions of the radiating bands obtained by combining Figs. 11<sub>a</sub> and 11<sub>b</sub> are compared with the observed ones reproduced from the original plate of Fig. 8, Plate I.<sup>1</sup> To compare these two positions, the direction represented by G in Figs. 11<sub>a</sub> and 11<sub>b</sub>, which nearly

1. It is to be noticed that the diffraction patterns reproduced in Plates I and II, are interchanged from right to left as compared with those of the original plate.



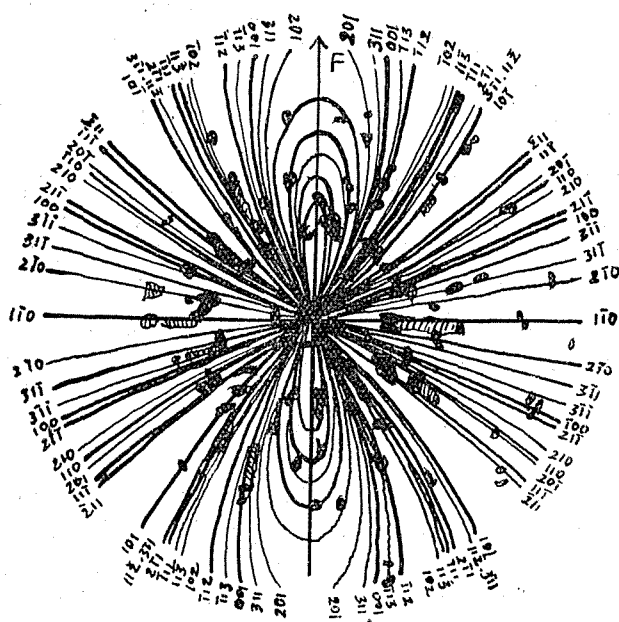


gested in Fig. 10, having one of their (110) planes in common, around the direction normal to this common plane; while, on the other hand, it is ascertained that the direction of the common axis above mentioned, is nearly parallel to the direction of the maximum growth of deposited tin. This seems to make clear the reason for the conclusion stated above.

Here it is noticed that the Specimens  $A_1$ ,  $A_2$  and  $A_3$  giving rise to the aforesaid diffraction patterns Figs. 6~8, Plate I, are of the comparatively simpler configurations among the specimens, which appeared from the electrolyte containing a small quantity of ferrous ions. With a few specimens belonging to the same category, patterns suggesting more complex configurations were also obtained, as reproduced in Fig. 9, Plate I. These diffraction figures being too complicated to be explained so minutely as before, the writers tried to find out only the gist of the corresponding crystalline configurations, by determining the common direction of the micro-crystals in some of the specimens of the exceptionally complex structures. This determination of the common direction could be made by comparing the diffraction patterns obtained by illuminating the incident X-ray beam on a specimen from its various directions, with the loci of the intensity maxima expected to be produced on the photographic plates in various cases, each one of these loci being given as the theoretical position of the radiating bands as confirmed by the crystallographic scale.

In the annexed figure, Fig. 13, the theoretical positions of the prominent radiating bands expected to be produced, when the incident beam was made to strike a fibrous aggregation of micro-crystals perpendicularly to their common direction, were compared with the diffraction pattern appearing in the original plate of Fig. 9, Plate I, which was obtained with Specimen  $A_4$  in the same way as those of Figs. 6~8, Plate I with Specimens  $A_1$ ,  $A_2$  and  $A_3$ . The above comparison was made by taking the direction of the maximum growth of deposited tin on the photographic plate G parallel to the common direction of micro-crystals F in the theoretical curves, which was assumed beforehand to coincide with one of the normals to (111) faces. As may be seen from this figure, the diffraction pattern observed on the photographic plate agrees well with the theoretical curves. Thus, it seems to be legitimate to presume that the micro-crystals of white tin in Specimen  $A_4$ , mostly arrange themselves having one of the normals to their (111) faces [instead of (110) faces as in Specimen  $A_1$ ,  $A_2$  and  $A_3$ ] in common.

Fig. 13



The above presumption deduced from Fig. 9, Plate I, was also found to be consistent with all the other diffraction patterns corresponding to the different orientations of Specimen A<sub>1</sub>. Fig. 14, Plate I shows the diffraction pattern taken with Specimen A<sub>1</sub>, when the longitudinal axis of this specimen was tilted 45° from its vertical position towards the incident beam. By examining the original plate of Fig. 14, Plate I, it could easily be seen that the diffraction pattern reproduced in Fig. 14 also agrees with the theoretical curves representing the prominent radiating bands, which were drawn by assuming that the common direction of micro-crystals was tilted 45° from its vertical position towards the incident beam, as seen in Fig. 15. Accordingly our foregoing presumptions being confirmed, we may conclude that the micro-crystals of white tin mostly arranged themselves in Specimen A<sub>1</sub>, each having one of the normals to its (111) faces in a definite common direction parallel to the longitudinal axis of the specimen. This is in no way different from the experimental results we previously obtained with electrolytic white tin deposited from solutions containing only stannic ions.

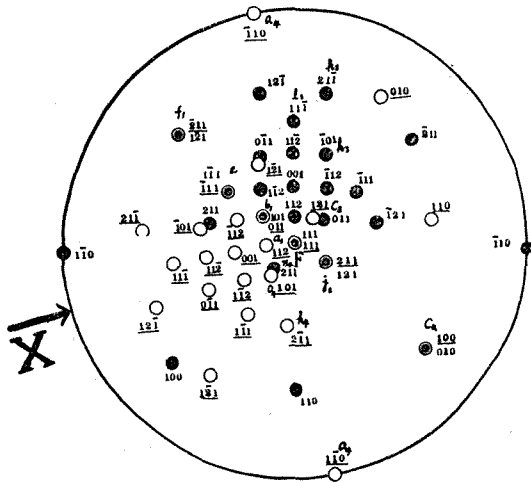
The arguments which have hitherto been advanced with regard to Specimen A, led us to conclude that even when the electrolyte



ign ions would be needed, as well as consideration of the metallographical and chemical properties of the metals concerned.

(ii) Specimen B. We consider next the effects of manganous ions in the electrolyte upon the inner structure of the electrolytic white tin. For this purpose, the crystalline configurations of Specimen B were also examined. By repeating the same procedure as in the cases of Figs. 6, 7, 8 and 9, Plate I, we obtained diffraction patterns consisting of a number of Laue spots as reproduced in Fig. 16, Plate II; however, in some of the patterns, these spots were found to be elongated. By calculating as before, it was concluded that the specimens giving rise to these figures are of a crystalline configuration entirely different from those of Specimen A (excepting Specimen A<sub>4</sub>): i. e., Specimen B is confirmed to be mostly composed either of two crystals of white tin having one of their (111) planes in common, or of an aggregation of micro-crystals arranged in a way that would result from the rotation of two such crystals around the direction normal to their

Fig. 17



common plane. And in both cases, this direction normal to the common plane is always found to be situated parallel to the direction of the maximum growth of the deposited tin. In Fig. 17, the orientation of white tin giving rise to Fig. 16, is represented in the same way of projection as in Fig. 9.<sup>1</sup> It can easily be seen from Fig. 17, that the crystalline configuration

1. The following correspondence was found to exist between the Laue spots in Fig. 16, Plate II and the atomic planes of the white tin crystals represented in Fig. 17:—

$a_1$ ,  $\bar{1}12$ ;  $b_1$ ,  $01\bar{1}$  &  $10\bar{1}$ ;  $c_1$ ,  $\bar{1}13$ ;  $d_1$ ,  $\bar{1}33$  &  $3\bar{1}3$ ;  $e_1$ ,  $\bar{1}1\bar{1}$  &  $1\bar{1}1$ ;  $f_1$ ,  $\bar{2}1\bar{1}$ ;  $g_1$ ,  $\bar{3}1\bar{1}$ ;  $h_1$ ,  $\bar{4}1\bar{1}$  &  $03\bar{1}$ ;  $a_2$ ,  $\bar{7}1\bar{1}$  &  $17\bar{1}$ ;  $b_2$ ,  $\bar{9}1\bar{1}$ ;  $c_2$ ,  $100$ ;  $f_2$ ,  $91\bar{1}$ ;  $g_2$ ,  $71\bar{1}$ ;  $h_2$ ,  $51\bar{1}$ ;  $i_2$ ,  $31\bar{1}$ ;  $j_2$ ,  $21\bar{1}$  &  $12\bar{1}$ ;  $k_2$ ,  $132$ ;  $l_2$ ,  $131$ ;  $m_2$ ,  $141$ ;  $n_2$ ,  $33\bar{1}$ ;  $o_2$ ,  $021$ ;  $a_3$ ,  $\bar{1}31$  &  $\bar{1}33$ ;  $b_3$ ,  $\bar{1}23$ ;  $c_3$ ,  $\bar{1}21$  &  $01\bar{1}$ ;  $d_3$ ,  $133$ ;  $e_3$ ,  $\bar{2}31$  &  $11\bar{1}$ ;  $f_3$ ,  $012$ ;  $g_3$ ,  $11\bar{5}$ ;  $h_3$ ,  $10\bar{1}$ ;  $i_3$ ,  $\bar{1}51$  &  $31\bar{3}$ ;  $j_3$ ,  $31\bar{2}$ ;  $k_3$ ,  $21\bar{1}$ ;  $l_3$ ,  $112$ ;  $m_3$ ,  $\bar{5}71$ ;  $n_3$ ,  $\bar{2}30$ ;  $o_3$ ,  $33\bar{1}$ ;  $q_3$ ,  $\bar{1}31$ ;  $a_4$ ,  $\bar{1}10$ ;  $b_4$ ,  $\bar{7}71$ ;  $c_4$ ,  $73\bar{1}$ ;  $d_4$ ,  $55\bar{1}$ ;  $e_4$ ,  $331$ ;  $f_4$ ,  $441$ ;  $g_4$ ,  $31\bar{1}$ ;  $h_4$ ,  $21\bar{1}$ ;  $k_4$ ,  $751$ ;  $l_4$ ,  $3\bar{1}1$ ;  $m_4$ ,  $53\bar{1}$ ;  $n_4$ ,  $313$  &  $211$ ;  $o_4$ ,  $101$ ;  $p_4$ ,  $313$ ;  $q_4$ ,  $312$ ;  $r_4$ ,  $717$ ;  $s_4$ ,  $213$  &  $311$ ;  $t_4$ ,  $751$ .

of Specimen B is not the same as that of Specimen A, nor is it like those of the electrolytic specimens of white tin deposited from stannous solutions free from any foreign metallic ion which were examined in our previous research. On the contrary, the crystalline configurations of Specimen B, which was deposited electrolytically from stannous solution containing a small quantity of manganous ions, were found to be more like those of the electrolytic specimens of white tin obtained with the stannic solutions free from any foreign metallic ion.

Here, it would be advisable to remark that the two binary phase diagrams formed by tin with iron and manganese respectively, were much alike.

(iii) Specimen C. The discussion up to this point has confined itself to electrolytic specimens of pure tin, deposited from various stannous solutions. But Specimen C which will now be dealt with was composed of 3.2% of Cu and 96.8% of Sn. Thus this specimen may be deemed a sort of eutectic alloy containing a considerable amount (nearly 10%) of the compound  $Cu_6Sn_5$ , at room temperature in its equilibrium state.

By repeating the experiment based upon the Laue method again, the diffraction patterns consisting of a number of Laue spots, as reproduced in Fig. 18, Plate II, were usually obtained with Specimen C. It can be confirmed by calculation, that these patterns were given rise to by essentially the same crystalline configuration as that of Specimen B, and consequently of the electrolytic specimens of white tin obtained with stannic solutions free from any foreign metallic ions. i. e., Specimen C may be said to be mainly composed of two crystals of two white tin having one of their (111) planes in common, and the normal to this common plane parallel to the direction of the maximum growth of the electrolytic deposition. In the annexed figure, Fig. 19, the crystalline configuration of Specimen C corresponding to Fig. 18, Plate II, is projected as in other cases.<sup>1</sup>

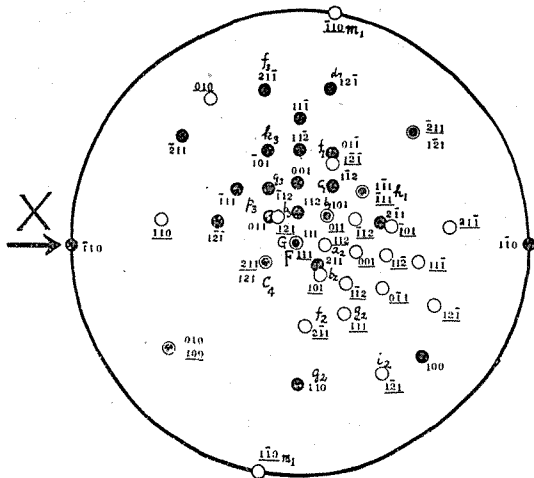
The facts above mentioned seem to suggest that a small quantity

---

1. The following correspondence was found to exist between the Laue spots in Fig. 18, Plate II and the atomic planes of the white tin crystals represented in Fig. 19:—

$a_1, 32\bar{1}$  &  $12\bar{3}$ ;  $b_1, 10\bar{1}$  &  $01\bar{1}$ ;  $c_1, 1\bar{1}2$ ;  $d_1, 12\bar{1}$ ;  $e_1, 13\bar{1}$ ;  $f_1, 01\bar{1}$  &  $12\bar{1}$ ;  $g_1, 03\bar{2}$  &  $2\bar{3}1$ ;  $h_1, 1\bar{1}1$  &  $1\bar{1}\bar{1}$ ;  $i_1, 03\bar{1}$ ;  $j_1, 3\bar{1}3$  &  $3\bar{3}\bar{1}$ ;  $k_1, 15\bar{1}$ ;  $m_1, 110$ ;  $n_1, 230$ ;  $o_1, 012$ ;  $p_1, 12\bar{3}$ ;  $a_2, 112$ ;  $b_2, 211$  &  $101$ ;  $c_2, 321$  &  $312$ ;  $d_2, 331$ ;  $e_2, 53\bar{1}$ ;  $f_2, 211$ ;  $g_2, 111$ ;  $h_2, 313$ ;  $i_2, 221$ ;  $j_2, 110$ ;  $k_2, 311$ ;  $l_2, 351$ ;  $a_3, 132$ ;  $b_3, 133$  &  $121$ ;  $c_3, 113$ ;  $d_3, 221$ ;  $e_3, 321$ ;  $f_3, 211$ ;  $g_3, 112$  &  $131$ ;  $h_3, 213$  &  $115$ ;  $k_3, 302$ ;  $l_3, 311$ ;  $o_3, 032$ ;  $p_3, 011$ ;  $b_4, 132$ ;  $c_4, 121$  &  $211$ ;  $d_4, 551$ ;  $f_4, 411$ ;  $k_4, 511$ ;  $l_4, 141$  &  $301$ ;  $n_4, 120$ ;  $q_4, 351$  &  $531$ ;  $s_4, 131$  &  $311$ ;  $t_4, 711$ .

Fig. 19



of cupric ions in the stannic solution have no remarkable effect upon the crystalline configuration of the electrolytic depositions. With regard to the state of copper atoms in Specimen C, it was conceived from the equilibrium diagram of the alloys belonging to Cu-Zn system, that the compound  $\text{Cu}_6\text{Sn}_5$  would be formed in this specimen, in the way that has been proved by Nakamura,<sup>1</sup> Dehlinger<sup>2</sup> and the present writers<sup>3</sup> utilizing some specimens of electrolytic brass ( $\alpha$ -solid solution belonging to Zn-Cu system), together with by Iwase<sup>4</sup> and the others<sup>5</sup> in the case of various electrolytic alloys belonging to the systems of Fe-Ni, Cu-Zn, Cd-Ag, Cd-Sn and Cd-Ni, etc. But no conclusive information could be deduced from our foregoing arguments in connection with Specimen C.

To make this point clear, the crystal structure of Specimen C was examined by means of the ordinary powder method. The powder photograph thus obtained with Specimen C was found, as may be seen in Fig. 20, Plate II, to lack even the lines due to the crystals of the compound  $\text{Cu}_6\text{Sn}_5$ , which may exist to a considerable amount (about 10%) in this specimen, not to speak of copper crystals: But it was observed to be entirely the same as the powder photograph of pure white tin. This shows us, contrary to the results of the previous investigation, that Specimen C consisting of two kinds of metals, tin and copper, is nothing but an aggregation of the crystals of white tin interspersed with colloidal particles containing copper atoms.

1. M. Nakamura; Scientific Rep. Institute Phys. and Chem. Research (Rikagaku Kenkyusho Iho), **4**, 71 (1926).

2. U. Dehlinger and F. Giesen; Zeits. f. Metallk., **24**, 197 (1932).

3. unpublished.

4. K. Iwase and N. Nasu; Bull. Chem. Soc. Japan, **7**, 305 (1932).

5. e. g., A. Roux and J. Cournot; Compt. rend. **186**, 1733 (1928).

### Conclusion

The arguments which have hitherto been advanced with regard to the electrolytic specimens deposited from stannous or stannic solutions containing foreign metallic ions, led us to the following conclusions :—

(1) The micro-crystals of white tin have a tendency to arrange themselves, in the electrolytic specimens deposited from the solutions containing  $Mn^{++}$  or  $Cu^{++}$  ions besides  $Sn^{++}$  or  $Sn^{++++}$  ions, with the normals to their (111) faces parallel to a definite common direction, as was found in our previous researches ; but with the specimens from solutions containing a small quantity of  $Fe^{++}$  ions in addition to  $Sn^{++}$  ions, this direction of the common axis was observed usually to coincide with the normals to (110) face of the micro-crystals of white tin.<sup>1</sup>

(2) The presence of  $Fe^{++}$  or  $Mn^{++}$  ions in addition to  $Sn^{++}$  ions in an electrolyte, not only converts the direction of the maximum growth of the deposited tin, in a way similar to the case of the alternation of the ionic valency of Sn, but also affects some other geometrical properties previously found with the electrolytic specimens of white tin.

(3) As the consequence of the experiment carried out with specimens consisting of Sn 96.8% and Cu 3.2%, it must be concluded, contrary to the results of our foregoing researches, that some electrolytic depositions containing two kinds of metals are nothing but an aggregation of crystals of one of these constituents, the other constituent being supposed to exist mostly in a colloidal state outside of the aforesaid crystals.

The facts summarized above seem to give some clues to the consideration of the effects of foreign metallic ions upon the inner structures of electrolytic metals and alloys.

In conclusion, the writers wish to express their sincere thanks to Professor Denzo Uno for his interest in the course of this investigation. Their thanks are also due to Dr. T. Nomitsu, who kindly supplied many specimens required, and to Mrs. M. Hara and S. Yoshimoto for their efficacious aid during the progress of the experiment.

Institute of Metallography,  
Kyoto Imperial University.

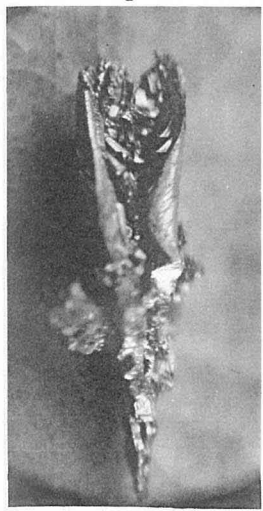
---

1. These two faces (111) and (110) here designated by Arkel's system, correspond respectively to (101) and (100) planes of the tetragonal white tin type lattice.



Plate I

Fig. 1



Specimen A<sub>1</sub>  
× 12

Fig. 2



Specimen A<sub>5</sub>  
× 12

Fig. 3



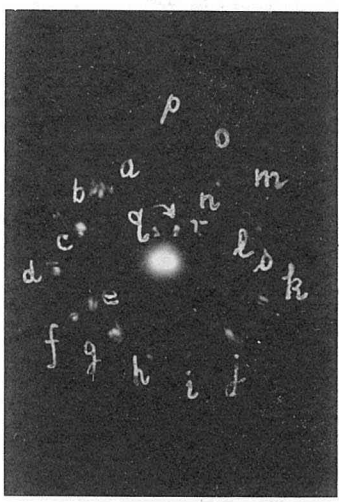
Specimen B<sub>1</sub>  
× 12

Fig. 4



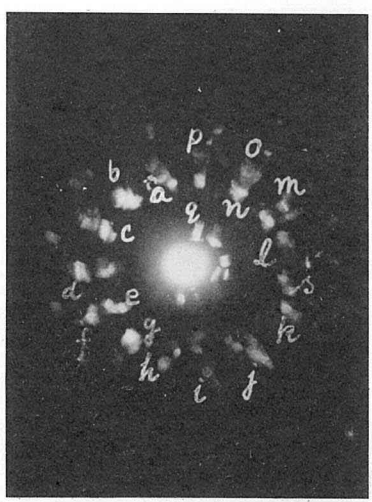
Specimen B<sub>3</sub>  
× 12

Fig. 6



Specimen A<sub>1</sub>

Fig. 7



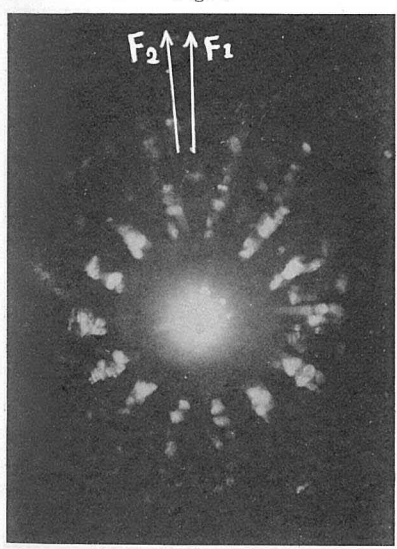
Specimen A<sub>2</sub>

Fig. 5



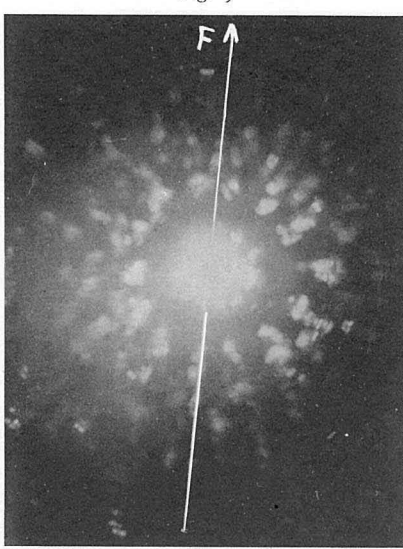
Specimen C  
× 85

Fig. 8



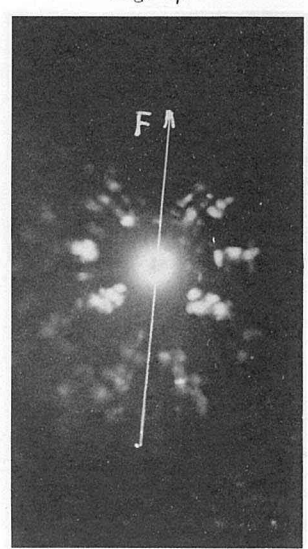
Specimen A<sub>3</sub>

Fig. 9



Specimen A<sub>4</sub>

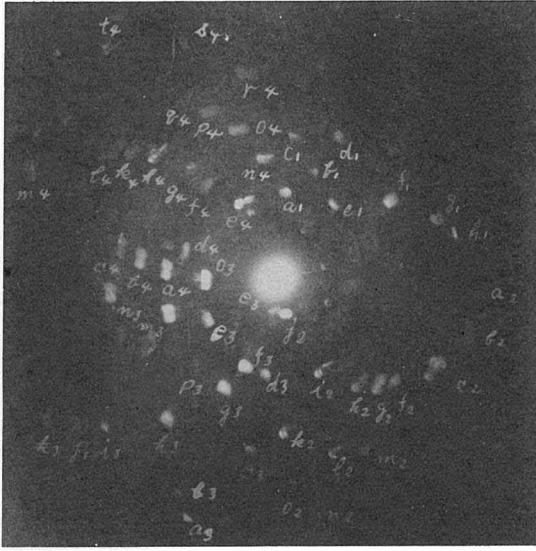
Fig. 14



Specimen A<sub>4</sub>

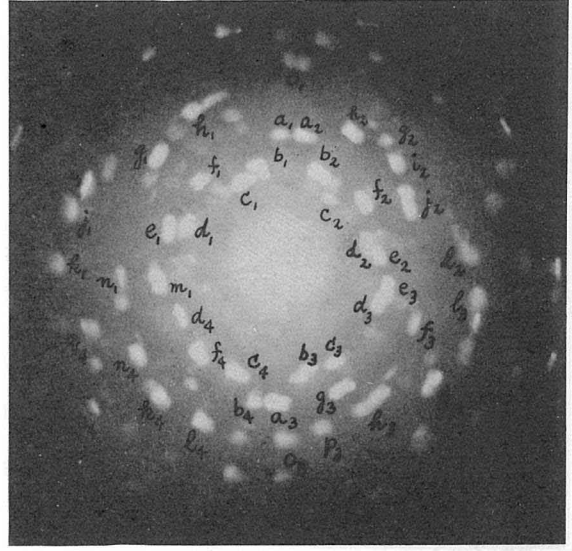
Plate II

Fig. 16



Specimen B<sub>1</sub>

Fig. 18



Specimen C

Fig 20

